

Interface and Bulk Fracture Modes and Strengths Determined by Laser-Induced Stress Pulses

Peter Hess and Alexey M. Lomonosov

Institute of Physical Chemistry, University of Heidelberg
Im Neuenheimer Feld 253, D-69129 Heidelberg; Germany
Tel: +49 6221 545205, Fax: +49 6221 544255
E-mail: peter.hess@urz.uni-heidelberg.de

ABSTRACT. *The quantitative determination of the mechanical strength of interfaces and solids by nonlinear acoustics with nanosecond lasers is reviewed. The pump-probe setups are described, which allow an all-optical contact-free excitation and detection of short elastic strain pulses. The development of shock pulses and the resulting impulsive failure in contact-free, notch-free, and mode-resolved manner (mode I+II+III) is described for film systems and anisotropic silicon. Strength values are presented for tensile and mixed-mode interfacial failure and for mode-resolved fracture by surface-breaking cracks for specific planes and directions in crystals.*

INTRODUCTION

To determine the mechanical strength of coatings or solids the loss of adhesion or fracture must be investigated. Versatile tools that often are used are the scratch tester, where a diamond stylus is drawn across the coated surface under increasing load to determine the critical load or the stylus is used as indenter. These methods are versatile but they are influenced by many factors such as substrate strength, film thickness and properties, and interface bonding and roughness. In addition, several test parameters such as scratching velocity and stylus properties affect the critical load. Due to the complexity of the processes with strongly inhomogeneous deformation fields, it is generally very difficult to extract quantitative values on the cohesion or fracture strength. This seems to be true for most widely used testing methods such as pull test, four point bend test, or blister test [1].

Quantitative information on the failure strength of materials can be obtained by laser techniques. Here a nanosecond laser pulse can be used to excite either bulk or surface acoustic stress pulses developing shocks during propagation. In these laser-based pump-probe methods a continuous wave (cw) laser probe is employed to measure the transient surface displacement or surface velocity. For bulk waves, mainly used to study interfacial strengths, the critical failure stress is determined from the surface distortion caused by the elastic pulse reflected at the film surface [2]. For surface acoustic waves (SAWs), employed to elucidate fracture modes of solids, the transient displacement or surface velocity of the pulse propagating along the surface is monitored at two locations [3]. The laser methods are contact-free and need no artificial seed crack to nucleate fracture because stresses of up to 10 GPa can be realized in relevant shock pulses.

EXPERIMENTAL

The quantitative investigation of fracture mechanics by laser ultrasonics is based on the efficient excitation of longitudinal, shear, and surface acoustic waves by strong nanosecond laser pulses. Especially, methods to use bulk stress pulses for delamination of films in mode I + II configuration have been developed [2,4-6].

The original method is based on laser excitation of longitudinal compressive waves on the side of the sample opposite to the film (see Fig.1). The nanosecond pulse of a Nd:YAG laser is collimated at the absorbing medium to an area of about 1-3 mm diameter [4]. Usually, the elastic pulse is generated by absorption of laser radiation in a 0.5 μm thick metal (Al) layer, which is sandwiched between the back side of the substrate and a ~ 10 μm thick transparent confining layer (SiO_2 , waterglass). Instead of an Al film as absorbing medium a 20 μm thick layer of silicone grease, containing fine MoS_2 particles, has been employed to excite stress waves by laser breakdown [5]. Tensile stress is generated when the compression pulse is reflected from the free surface. At the surface the resulting stress is zero and reaches its maximum at a distance equal to half of the spatial pulse extension. This restricts the thickness of the films to be delaminated. The situation can be improved by modifying the shape of the stress pulse using an unusual nonlinear property of fused silica, which develops a shock at the tail of the pulse for compressive stresses below 4 GPa (rarefaction shock) [2]. In this case the tensile stress reaches its maximum at a distance of the width of the post-

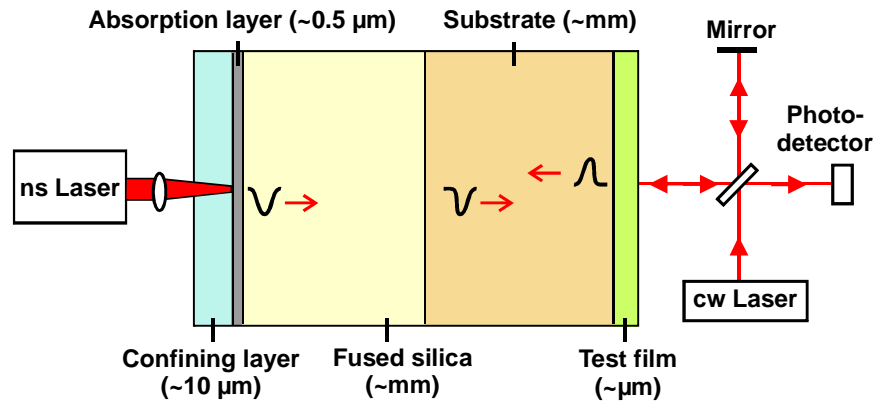


Fig.1 Setup for tensile interfacial spallation with a pulsed laser, substrate with test film, layers for shock wave formation, and interferometer to monitor the film surface [4].

peak shock, making the method applicable for significantly thinner films. From measurements of the transient out-of-plane displacement or velocity of the free film surface at the epicenter by a laser interferometer the interfacial strength is obtained for specular and diffuse surfaces using a cw laser [6].

Besides longitudinal stress pulses shear pulses can be generated by using a triangular fused silica prism for mode conversion of the excited longitudinal compressive wave into a shear wave upon oblique incidence onto a surface, as illustrated in Fig. 2 [7-9]. With such a setup nearly complete conversion into high amplitude shear pulses, and therefore mode II fracture by in-plane shear stress can be achieved at a prism angle of $\theta = 57.7^\circ$ [8]. Consequently, mixed-mode loading is possible and it is important to note that in most practical situations thin films tend to fail under mixed-mode I + II conditions.

SAWs are guided waves, which penetrate approximately one wavelength deep into solids. Thus, the main part of the elastic energy stays within this depth during wave propagation along the surface. Note that these elliptically polarized waves possess both a longitudinal and shear component. In the pump-probe setup a pulsed laser is employed to launch nanosecond SAW pulses with finite amplitudes, which develop shocks during propagation. A distinctive property of SAWs is their intrinsic tensile stress, or its generation during nonlinear evolution. A cw laser is used for detection of the moving pulses at two surface locations [3].

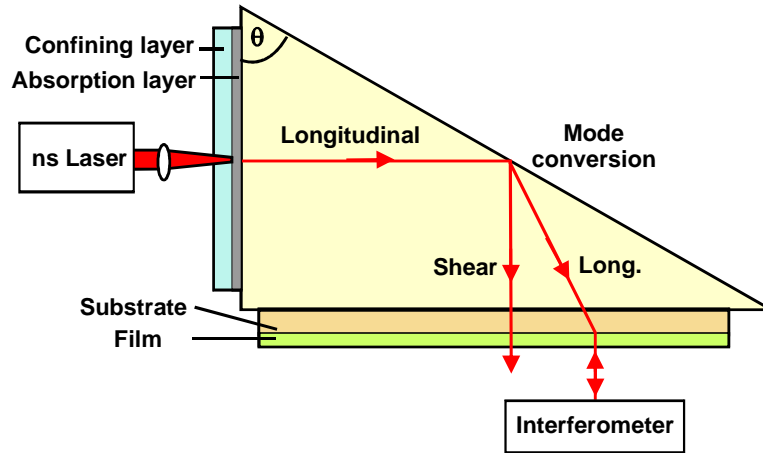


Fig. 2 Setup for shear stress delamination with a pulsed laser, fused-silica prism for mode conversion, and interferometer to monitor the film surface [8].

Typically, a Nd:YAG laser radiating at $1.064 \mu\text{m}$ with 30-160 mJ pulse energy and 8 ns pulse duration is applied in single-pulse experiments. As depicted in Fig. 3, the explosive evaporation of a thin layer of a highly absorbing carbon suspension, deposited only in the source region, is used to launch SAW pulses with finite amplitude. By sharply focusing the pump laser pulse with a cylindrical lens into a line a plane surface wave propagating in a well-defined direction is launched. If the shock formation distance is smaller than the attenuation length a propagating SAW pulse with finite amplitude develops a steep shock front. These nonlinear SAW pulses gain amplitudes of 100-200 nm, as compared with few nanometers for linear SAWs. The shape of the pulse with finite amplitude changes due to frequency-up and frequency-down conversion processes, caused by the elastic nonlinearity of the solid. The profile of the transient surface displacement can be detected with a stabilized Michelson interferometer [3]. In most cases, however, the more versatile transient deflection of a cw probe-laser beam is monitored by a position-sensitive detector, to determine the surface velocity or shear displacement gradient [3]. In the two-point-probe scheme the SAW profile is registered at 1-2 mm and 15-20 mm distance from the line source. The pulse shape measured at the first probe spot is inserted as initial condition in the nonlinear evolution equation to simulate the development of the SAW pulse nonlinearity and to verify agreement between theory and experiment.

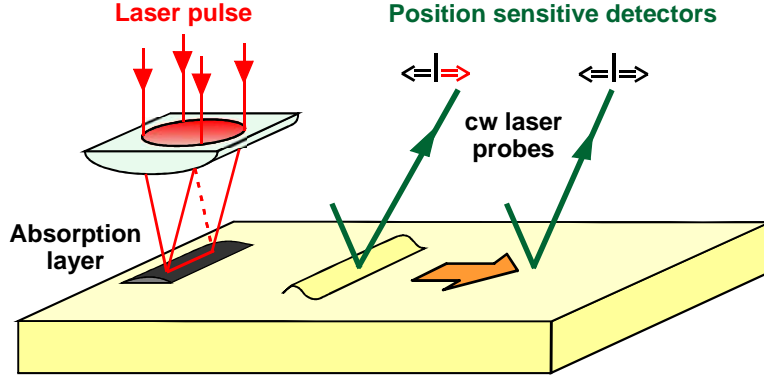


Fig. 3 Setup for exciting plane SAW pulses with shocks and two-point cw probe-laser deflection to monitor the surface velocity [3].

RESULTS ON INTERFACIAL DECOHESION WITH BULK WAVES

Up to now in most bulk experiments longitudinal pulses have been used for spatially localized delamination of films in the irradiated area by pure tensile stresses (mode I). As mentioned before, the tensile stress pulse reflected at the free film surface is responsible for the local complete removal (spallation) of the film. Interferometric measurement of the transient surface displacement u yields the following stress acting on the interface in one-dimensional approximation

$$\sigma_{\text{int}}(h,t) = (1/2)(\rho c_f) [v(t + h/c_f) - v(t - h/c_f)] \quad (1)$$

where ρ is the density of the film, h is the film thickness, c_f the longitudinal speed of the stress wave in the film, and $v = \partial u / \partial t$ [10].

In the case of very thin films, the reflected tensile pulse may overlap with the incoming compressive pulse, reducing the effective stress at the interface. In this situation it can happen that first the critical fracture strength of the substrate is reached at a certain penetration depth of the tensile pulse into the substrate. By increasing the film thickness the incoming and reflected pulse can be separated leading to film spallation. Such a behavior has been observed for silicon covered by a bilayer of TaN/Cu. The TaN layer thickness was fixed to 20 nm, whereas the Cu layer was varied between 100 nm and 10 μm . At a Cu-layer thickness $\leq 1 \mu\text{m}$

silicon fracture with an intrinsic tensile strength of ~5 GPa was observed. At a Cu-layer thickness of $\geq 5 \mu\text{m}$ the Si/TaN interface was debonded at 1.4 GPa [10].

Mixed-mode failure was studied in comparison with pure mode I for a silicon wafer (730 nm) covered with a Si_xN_y passivation layer (400 nm) and an Au film of different thicknesses (300 nm, 600 nm, and 1200 nm) [9]. The back side of the silicon substrate was bonded to a fused silica prism equipped with an Al layer (400 nm) and a confining waterglass layer. For the pure tensile strength between Au film and passivated Si substrate a critical stress of 245 MPa was found. Under mixed-mode conditions, delamination was observed for ~142 MPa tensile and ~436 MPa shear stress. Thus, by applying the shear load the strength was reduced by ~100 MPa. The effective stress in the mixed-mode case was ~449 MPa [9]. An interpretation of this finding is that mixed-mode delamination consumes more energy. While the method yields mode-resolved strengths, the stress fields generated by conventional scratch, peel, pull, blister, and indentation tests are difficult to analyze quantitatively due to inhomogeneities and plastic deformation.

Recently, the spallation and fracture of bulk polycrystalline tungsten and of a tungsten/tungsten interface, produced by magnetron sputtering of a tungsten film, was studied [11]. While for bulk tungsten a strength of 2.7–3.1 GPa was found, the interfacial strength was only 875 MPa.

RESULTS ON MODE-RESOLVED FRACTURE BY SURFACE WAVES

With SAWs high nonlinearities and strains can be realized easier than with bulk waves [12]. The potential of SAWs in resolving multi-mode fracture processes is demonstrated here for single-crystal silicon. Surface-breaking microcracks of $<100 \mu\text{m}$ length and $<50 \mu\text{m}$ depth were induced by intrinsic surface nucleation with SAWs propagating along defined crystallographic planes and directions (geometries). Pure mode I fracture occurs for cleavage planes normal to both the free surface and the propagation direction. Normally, fracture has a multimode character (modes I+II+III) with several relevant stress components.

The profiles of the SAW pulses registered at the second probe spots were simulated by solving the nonlinear evolution equation

$$i \frac{\partial}{\partial \tau} B_n = nq_0 \left[\sum_{0 < n' < n} F(n'/n) B_{n'} B_{n-n'} + 2 \sum_{n' > n} (n/n') F^*(n/n') B_{n'} B_{n'-n}^* \right] \quad (2)$$

where B_n is the n -th harmonic of the signal, τ the stretched coordinate along wave propagation, q_0 the fundamental wave number, and $F(x)$ a dimensionless function. This function describes the efficiency of frequency conversion and depends on the ratio of the second-order to third-order elastic constants of the selected geometry. For example, $F(1/2)$ describes the efficiency of second harmonic generation. Calibration of the evolution equation, using the measured signal of the first probe spot, allows the extraction of the critical fracture stress at the locations, where cracks are observed [13].

An interesting totally unexpected observation was that counterpropagating nonlinear SAW pulses, moving in opposite directions, e.g., in the $\langle -1-12 \rangle$ and the $\langle 11-2 \rangle$ directions on the Si(111) plane, develop completely different nonlinear pulse shapes [12]. As a consequence of this nonlinear effect, fracture can be induced with much lower laser-pulse energies in the “easy cracking” $\langle -1-12 \rangle$ direction. For particular silicon geometries the propagation of the shocked SAW pulse introduced a whole crack field of about 50–100 μm long cracks by repetitively fracturing the crystal after a certain propagation distance. Cracking occurred perpendicular to the SAW propagation direction and normally extended along one of the weakest Si{111} cleavage planes into the bulk.

This procedure provided, e.g., values of the critical tensile stress components for low index plane geometries of 2–7 GPa [14,15]. This agrees with the strength of ~ 5 GPa obtained for an undefined geometry by longitudinal stress pulses [10]. Several multi-mode fracture processes were characterized in anisotropic silicon.

CONCLUSIONS

Laser-induced stress pulses provide a novel efficient tool to elucidate the mode-specific delamination of films. Here the shock-pulse method measures the intrinsic interface strength. In anisotropic crystals intrinsic surface nucleation and multi-axial fracture can be studied. The defined loading geometries realized with bulk and surface waves allow a straightforward interpretation. These methods provide important insight into pure mode but also multi-mode failure. In fact, the critical stress or failure strength of spallation, delamination, and fracture can be determined in layered and anisotropic materials. For high-quality materials such as single-crystal silicon the measured critical stress components can be compared with *ab initio* calculations, performed for defined fracture geometries, to judge the

mechanical quality of real materials. Owing to the high strain rates ($\sim 10^6 \text{ s}^{-1}$) involved, the influence of plastic deformations is reduced. This usually allows a more sensitive and accurate analysis of the mechanical strength, which is of increasing interest in thin film technology and device fabrication. First interesting results on the mechanical response of MEMS structures have been reported [16].

REFERENCES

- [1] Lacombe, R.H. (2006) *Adhesion Measurement Methods: Theory and Practice*, CRC Press, Boca Raton.
- [2] Wang, J., Weaver, R.L. and Sottos, N.R. (2003) *J. Appl. Phys.* **93**: 9529-9536.
- [3] Lomonosov, A.M., Mayer, A.P. and Hess, P. (2001). In: *Modern Acoustical Techniques for the Measurement of Mechanical Properties*, Levy, M., Bass, H. E. and Stern, R. Eds., Academic, San Diego, pp. 65-134.
- [4] Gupta, V., Argon, A.S., Cornie, J.A. and Parks, D.M. (1990) *Materials Science and Engineering A* **126**: 105-117.
- [5] Ikeda, R., Cho, H., Sawabe, A. and Takemoto, M. (2005) *Diamond and Rel. Mat.* **14**: 631-636.
- [6] Pronin, A.N. and Gupta, V. (1993) *Rev. Sci. Instrum.* **64**: 2233-2236.
- [7] Wang, J., Sottos, N.R. and Weaver, R.L. (2003) *Experimental Mechanics* **43**: 323-330.
- [8] Hu, L. and Wang, J. (2006) *Experimental Mechanics* **46**: 637-645.
- [9] Kitey, R., Geubelle, P. H. and Sottos, N.R. (2009) *J. Mech. Phys. Solids* **57**:51-66.
- [10] Gupta, V., Kireev, V., Tian, J., Yoshida, H. and Akahoshi, H. (2003) *J. Mech. Phys. Solids* **51**: 1395-1412.
- [11] Hu, L., Miller, P. and Wang, J. (2009) *Materials Science and Engineering A* **504**: 73-80.
- [12] Lomonosov, A.M. and Hess, P. (2002) *Phys. Rev. Lett.* **89**:095501-1-4.
- [13] Lehmann, G., Lomonosov, A.M., Hess, P. and Gumbsch, P. (2003) *J. Appl. Phys.* **94**: 2937-2941.
- [14] Kozhushko, V.V., Lomonosov, A.M. and Hess, P. (2007) *Phys. Rev. Lett.* **98**: 195505-1-4.
- [15] Kozhushko, V.V. and Hess, P. (2007) *Phys. Rev. B* **76**: 144105-1-11.
- [16] Kimberley, J., Chasiotis, I. and Lambros, J. (2008) *Int. J. Solids Struct.* **45**: 497-512.